DALTON
FULL PAPER

The affinity and selectivity of terdentate nitrogen ligands towards trivalent lanthanide and uranium ions viewed from the crystal structures of the 1 : 3 complexes

Jean-Claude Berthet,*[a] Yannick Miquel,[a] Peter B. Iveson,[a] Martine Nierlich,[b] Pierre Thuéry,[b] Charles Madic[c] and Michel Ephritikhine*[a]

[a] *Laboratoire de Chimie de Coordination, Service de Chimie Moléculaire, DSM, DRECAM, CNRS URA 331, CEA/Saclay, 91191 Gif-sur-Yvette, France. E-mail: ephri@drecam.cea.fr*
[b] *Laboratoire de Cristallochimie, Service de Chimie Moléculaire, DSM, DRECAM, CNRS URA 331, CEA/Saclay, 91191 Gif-sur-Yvette, France*
[c] *DEN, CEA/Saclay, 91191 Gif-sur-Yvette, France*

Received 17th April 2002, Accepted 13th June 2002
First published as an Advance Article on the web 23rd July 2002

Treatment of LnI_3 (Ln = La, Ce) or $[UI_3(py)_4]$ with 3 equivalents of terpy in acetonitrile gave the tris(terpy) complexes $[M(terpy)_3]I_3$. Addition of 3 equivalents of Rbtp (2,6-bis(5,6-dialkyl-1,2,4-triazin-3-yl)pyridine) to MX_3 (X = I or OSO_2CF_3) in pyridine or acetonitrile afforded the tris(Rbtp) compounds $[M(Rbtp)_3]X_3$. By comparison with terpy, the Rbtp ligand has a better affinity for the 4f and 5f ions and is more selective for U(III) than for Ce(III) or La(III). This trend has been revealed by ^{1}H NMR competition experiments and X-ray crystallographic studies which show that in the $[M(terpy)_3]^{3+}$ and $[M(Rbtp)_3]^{3+}$ cations, the M–N(Rbtp) bond lengths are shorter than the M–N(terpy) bond lengths, and the U–N bond lengths are shorter than the corresponding Ce–N or La–N bond distances.

Introduction

Trivalent lanthanide (Ln) and actinide (An) ions exhibit strong analogies in their chemical properties and their clear differentiation, which is highly desirable and potentially useful in various areas, from biology to materials science, represents a difficult challenge.[1,2] Such a discrimination between Ln(III) and An(III) complexes implies the precise knowledge and control of their distinctive particularities, in connection with the accurate description of the metal–ligand bond and the respective involvement of the 4f and 5f electrons. In coordination chemistry, the selective complexation of actinides(III) over lanthanides(III) with efficient extractant molecules is an important problem for both its fundamental aspects and its applications, in particular in the partitioning of spent nuclear fuels.[3,4]

Differences in the coordinating ability of any given ligand towards trivalent 4f and 5f ions is related to the distinct formation constants of the corresponding analogous complexes and can be revealed by significant variations in the structural parameters of these complexes. Brennan *et al.* found that in the pairs of isostructural organometallic compounds $[U(C_5H_4Me)_3(L)]$ [M = Ce or U; L = $N(CH_2CH_2)_3CH$, PMe_3, $P(OCH_2)_3CEt$], the Ce–N and U–N bond lengths are the same whereas the U–P bond lengths are shorter than the Ce–P bond lengths.[5] While the Ce(III) and U(III) ions have similar sizes, the shortening of the U–P relative to the Ce–P bond corresponds to the observed greater stability of the alkylphosphine and phosphite complexes of uranium in solution, and was explained by a π back-bonding interaction between the uranium atom and the phosphorous ligand which is less likely in the lanthanide complex. The better π-donor capacity of the trivalent uranium metallocenes was further demonstrated by IR studies of the corresponding isocyanide adducts, and also by the formation of carbon monoxide complexes of uranium, but not of cerium, in which the IR frequency ν_{CO} is lowered upon coordination.[6]

As an extension to this pioneering work, attention was then paid to the complexation of the less electron rich metal species MX_3 (M = Ln, U; X = I, ClO_4, OSO_2CF_3) with neutral polydentate nitrogen Lewis bases, in particular those which were found to be efficient in the An(III)/Ln(III) separation by liquid–liquid extraction. A limited number of analogous compounds of U(III) and La(III) or Ce(III) with such ligands have been crystallographically characterized: $[M(Mentb)_2]X_3$ [M = La and X = ClO_4,[7] M = U and X = I;[8] Mentb = tris(*N*-methylbenzimidazol-2-ylmethyl)amine], $[MI_3(tpa)(py)]$ [M = La or U; tpa = tris[(2-pyridyl)methyl]amine; py = pyridine],[8] $[MI_3(bipy)_2(py)]$ (M = Ce or U; bipy = 2,2′-bipyridine)[9] and $[M(Pr^nbtp)_3]I_3$ [M = Ce or U; Rbtp = 2,6-bis(5,6-dialkyl-1,2,4-triazin-3-yl)pyridine].[10] In the first three compounds, the difference between the average U–N(polydentate ligand) and Ln–N(polydentate ligand) is less than 0.02 Å and can be considered as not significant in view of the experimental errors; this corresponds to the poor selectivity of these nitrogen Lewis bases in the An(III)/Ln(III) separation. In contrast, the U–N bond lengths are significantly shorter than the Ce–N bond distances in the $[M(Pr^nbtp)_3]^{3+}$ cations, in line with the remarkable capacity of Rbtp molecules to coordinate trivalent actinides in preference to trivalent lanthanides.[11]

In the presence of an organic acid as a synergist, the terdentate ligand 2,2′:6′,2″-terpyridine (terpy) also exhibits a better affinity for An(III) *vs.* Ln(III), although much less pronounced than btp.[11] It seemed of interest to determine whether the distinct coordinating abilities of these geometrically similar extractant molecules would correlate with the metal–nitrogen bond distances in their 4f and 5f metal complexes. Very recently, the first terpy complex of uranium, $[UI_2(terpy)_2(py)]I$, was isolated and the crystal structure of a pyridine solvate showed that the mean U–N(terpy) bond distance is 0.05 Å shorter than the Ce–N(terpy) bond length in the cerium compound $[CeI_2(terpy)_2(OH_2)]I$; this difference reveals the possible relation between the metal–nitrogen bond length and

DOI: 10.1039/b203725d

the selectivity of the terdentate ligand.[12] Here we present the synthesis and X-ray crystal structures of the isostructural tris(terpy) compounds $[M(terpy)_3]I_3 \cdot 2MeCN$ (M = La, Ce, Nd, U); these structures are compared with those of the tris(Rbtp) complexes $[M(Pr^nbtp)_3]I_3 \cdot npy$ (M = Ce and n = 3; M = U and n = 4) which have been previously reported,[10] and of the new complexes $[M(Mebtp)_3][OTf]_3 \cdot MeCN$ (M = La or Ce; OTf = OSO_2CF_3) and $[Ce(Mebtp)_3][OTf]_2I \cdot 2py$.

Results and discussion

Formation of the tris(terpy) complexes

We recently reported that addition of 2 equivalents of terpy to a pyridine solution of MI_3 (M = Ce, Nd) or $[UI_3(py)_4]$ gave the bis(terpy) compounds $[MI_2(terpy)_2]I$ (M = Ce, Nd) or $[UI_2(terpy)_2(py)]I$ in almost quantitative yield.[12] These complexes were stable in pyridine in the presence of an excess of terpy and no exchange was observed between the free and coordinated ligand. The lanthanide tris(terpy) complexes $[Ln(terpy)_3]I_3$ [Ln = La (**1**), Ce (**2**) and Nd (**3**)] were synthesized from a 1 : 3 mixture of LnI_3 and terpy in acetonitrile. The mixture was heated under reflux for 2 h and the product was isolated after filtration as a yellow–orange microcrystalline powder; the yields varied from 78 to 85%. The same reaction with $[UI_3(py)_4]$ was performed at room temperature in order to avoid the formation of an unidentified ochre oxidation product; after filtration and washing with toluene, the dark green powder of $[U(terpy)_3]I_3$ (**4**) was obtained in 85% yield. Complexes **1**–**4** were transformed in pyridine into the corresponding bis(terpy) compounds, with liberation of a terpy molecule. It is clear that acetonitrile, being a less coordinating and more polar solvent than pyridine, favours the coordination of the terpy ligand and the dissociation of the iodide ion, and allows the formation of the tris(terpy) complexes. It is always with the weakly coordinating perchlorate anion that the only other tris(terpy) complexes of the f elements $[M(terpy)_3][ClO_4]_3$ (M = Ce, Eu, Lu),[13,14] $[M(Rterpy)_3][ClO_4]_3$ (M = La, Eu, Tb; Rterpy = 4-Et or 4-Bu^t-terpy)[15] and Eu(III) complexes of polymethylene bridged derivatives of terpy[16] were prepared in acetonitrile or ethanol solutions. The crucial role of the counter ion was also illustrated by the formation of a mixture of bis and tris(terpy) complexes upon addition of an excess of terpy to a solution of the triflate compounds $M(OTf)_3$ in acetonitrile; this result confirms that the triflate ligand in f element complexes is much less easily displaced than the iodide and perchlorate.[17] The synthesis and structure of the bis(terpy) complexes $[M(OTf)_2(terpy)_2(py)](OTf)$ (M = Ce, Nd, U) will be presented in a forthcoming paper.

In contrast to their perchlorate and triflate analogues, the iodide complexes **1**–**4** are poorly soluble in acetonitrile and quite insoluble in tetrahydrofuran or benzene. The ^{1}H NMR spectra of **1**–**3** in CD_3CN exhibit the set of resonances corresponding to equivalent terpy ligands in a D_3 symmetrical arrangement. Satisfactory elemental analyses (C, H, N) were obtained for compounds **1**–**4**. The X-ray crystal structures of the acetonitrile solvates $[M(terpy)_3]I_3 \cdot 2MeCN$ (M = La, Ce, Nd, U) and $[Ce(terpy)_3]I_3 \cdot 3MeCN$ have been determined (*vide infra*).

Formation of the tris(Rbtp) complexes

It has been recently shown that addition of Rbtp molecules to the nitrate salts of the late lanthanides (Sm, Tm, Yb) in ethanol gives the $[Ln(Pr^nbtp)_3]^{3+}$ cations[18] while only the mono and bis(Rbtp) complexes $[Ln_2(Mebtp)_2(NO_3)_6]$ (Ln = Nd, Pr), $[Nd(Etbtp)(NO_3)_3(EtOH)]$ and $[Nd(Bu^ibtp)_2(NO_3)_2][Nd(NO_3)_5]$ are obtained with the early lanthanides.[19] The synthesis of the tris(Rbtp) compounds of the larger lanthanides(III) and uranium(III) ions would be possible by using less coordinating solvents and counterions. Indeed, the preparation of $[Ce(Rbtp)_3]I_3$ [R = Me (**5**) and Pr^n (**6**)] and $[U(Pr^nbtp)_3]I_3$ (**7**) was achieved from the metal iodides and Rbtp in pyridine.[10] These complexes were also obtained in acetonitrile, and the triflate analogues $[M(Mebtp)_3][OTf]_3$ [M = La (**8**), Ce (**9**), U (**11**)] were synthesized by addition of 3 equivalents of Mebtp to $M(OTf)_3$ in pyridine or acetonitrile. After evaporation of the solvent, washing with toluene and crystallization from pyridine, the complexes were isolated as yellow–orange (La, Ce) or gray–blue (U) powders. Complexes **8**, **9** and **11** have been characterized by their elemental analyses (C, H, N) and their ^{1}H NMR spectra which exhibit four resonances in the intensity ratio of 18 : 18 : 6 : 3 corresponding to three equivalent Mebtp ligands in a D_3 symmetrical arrangement. It is interesting to note that the spectrum of **9** in C_5D_5N is slightly different from that of its iodide analogue **5**, the paramagnetic shifts of the signals being larger by *ca.* 1.5 ppm. The spectrum of an equimolar mixture of **5** and **9** exhibits signals with chemical shifts intermediate between those of **5** and **9**, and the same spectrum was observed by adding 3 equivalents of KOTf to a pyridine solution of **5**. These results suggest the presence of some interaction in solution between the $[Ce(Mebtp)_3]^{3+}$ cation and the OTf^- anion. Crystals of $[Ce(Mebtp)_3][OTf]_2I \cdot 2py$ (**10**·2py) were deposited from the solution of **5** and **9**, and their structure was determined by X-ray diffraction analysis, as well as the crystal structures of acetonitrile solvates of **8** and **9** (*vide infra*).

Competition reactions

Formation of the tris(terpy) and tris(Rbtp) complexes **1**–**11** confirms that these terdentate ligands have a good affinity for the 4f and 5f ions. However, in contrast to the tris(terpy) compounds, the tris(Rbtp) analogues could be readily prepared in pyridine solvent and from the triflates $M(OTf)_3$, showing that Rbtp is more efficient than terpy in the competition reaction with the coordinating solvent and counter ions. The much better affinity of Mebtp than terpy for the trivalent 4f and 5f ions was further demonstrated by competition experiments. Thus, addition of 3 equivalents of Mebtp to $[Ce(terpy)_3]X_3$ (X = I or OTf) in pyridine or acetonitrile led to the quantitative formation of $[Ce(Mebtp)_3]X_3$. In the presence of 3 equivalents each of terpy and Mebtp, $[UI_3(py)_4]$ was totally transformed in pyridine into $[U(Mebtp)_3]I_3$. The capacity of the terdentate ligands to coordinate trivalent actinides in preference to trivalent lanthanides was illustrated by their competition reactions with Ce(III) and U(III). In the presence of 2 mol equivalents of terpy in pyridine, a 1 : 1 mixture of CeI_3 and $[UI_3(py)_4]$ was transformed into $[CeI_2(terpy)_2]I$ and $[UI_2(terpy)_2(py)]I$ in the molar ratio of 1 : 3.[12] Addition of 3 equivalents of terpy to a 1 : 1 mixture of the cerium and uranium triiodides in acetonitrile gave the corresponding bis and tris(terpy) compounds, but the insolubility of the latter impeded the determination of selectivity. Most notably, addition of 3 mol equivalents of Mebtp to 1 mol equivalent of both CeI_3 and $[UI_3(py)_4]$ in pyridine gave only $[U(Mebtp)_3]I_3$; no cerium complex could be detected.[10] These results are in agreement with the selectivity factors measured in the Am(III)/Eu(III) separation with Rbtp ligands from aqueous nitric acid solutions, which lie between 50 and 150 and are ten times greater than those observed with terpy and its derivatives. Moreover, the Rbtp ligands do not require the use of a synergist such as 2-bromodecanoic acid which is necessary in liquid–liquid extractions with terpy.[11]

The distinct affinities of terpy and Rbtp molecules for Ln(III) and U(III), as well as the distinct selectivities of these terdentate ligands for U(III) over Ln(III), could be assessed through the crystal structures of their analogous complexes.

Crystal structures of the complexes

Crystals of acetonitrile or pyridine solvates of the tris(terpy) compounds **1**–**4** and tris(Rbtp) complexes **5**–**10** are composed

Table 1 Selected bond lengths (Å) and angles (°) in the tris(terpy) complexes

	[La(terpy)$_3$]I$_3$·2MeCN **1**·2MeCN	[Ce(terpy)$_3$]I$_3$·2MeCN **2**·2MeCN	[Ce(terpy)$_3$]I$_3$·3MeCN **2**·3MeCN	[Nd(terpy)$_3$]I$_3$·2MeCN **3**·2MeCN	[U(terpy)$_3$]I$_3$·2MeCN **4**·2MeCN
M–N(1)	2.639(3)	2.613(3)	2.646(5)	2.587(3)	2.592(5)
M–N(2)	2.683(3)	2.657(3)	2.674(7)	2.618(3)	2.625(5)
M–N(3)	2.654(3)	2.626(3)		2.617(3)	2.622(5)
M–N(4)	2.719(3)	2.695(3)		2.676(3)	2.679(5)
M–N(5)	2.689(4)	2.667(5)		2.637(5)	2.622(7)
⟨M–N$_c$⟩	2.686(4)	2.662(7)	2.674(7)	2.63(1)	2.623(2)
⟨M–N$_l$⟩	2.67(4)	2.64(4)	2.646(5)	2.63(4)	2.63(4)
N(1)–M–N(2)	61.60(9)	62.06(10)	62.45(13)	62.61(10)	62.89(16)
N(2)–M–N(3)	61.79(9)	62.33(10)		63.09(10)	62.57(15)
N(1)–M–N(3)	123.33(9)	124.34(11)	124.9(3)[c]	125.65(11)	125.42(15)
N(4)–M–N(5)	60.64(6)	61.09(7)		61.66(7)	61.58(11)
N(4)–M–N(4′)	121.28(13)	122.19(14)		123.33(15)	123.2(2)
$\theta_{c,l}$[a]	3.6(2), 17.7(2)	3.9(3), 17.8(2)	16.7(4)	4.3(2), 18.3(2)	4.4(4), 18.1(3)
	24.0(3)	24.2(2)		24.3(2)	24.0(3)
$\theta_{l,l}$[b]	19.9(2)	19.9(2)	32.1(3)	20.7(2)	20.5(3)
	46.8(1)	47.0(1)		47.6(1)	47.2(2)

[a] With the exception of the trigonal compound **2**·3MeCN, are given successively the two $\theta_{c,l}$ angles in the terpy ligand defined by N(1), N(2) and N(3), and the $\theta_{c,l}$ angle in the terpy ligand defined by N(4) and N(5). [b] With the exception of the trigonal compound **2**·3MeCN, are given successively the $\theta_{l,l}$ angle in the terpy ligand defined by N(1), N(2) and N(3), and the $\theta_{l,l}$ angle in the terpy ligand defined by N(4) and N(5). [c] N(1)–Ce–N(1′) angle.

of discrete $[M(terpy)_3]^{3+}$ or $[M(Rbtp)_3]^{3+}$ cations, I^- or OTf^- anions and solvent molecules. In the cations, the metal centres are nine coordinate in a slightly distorted *mer*-tricapped trigonal prismatic configuration which is classical for complexes of general formula M(terdentate ligand)$_3$.[20] The capping positions are occupied by the nitrogen atoms N_c of the central pyridine rings [N(2) and N(5) in terpy, N(1) in Rbtp], whereas the trigonal bases are defined by the nitrogen atoms N_l of the lateral pyridine rings in terpy [N(1), N(3) and N(4)] or at the 2 position of the triazine rings in Rbtp [N(3) and N(6)]. A line-drawing showing the tricapped-trigonal-prismatic coordination of the complexes is shown in Fig. 1.

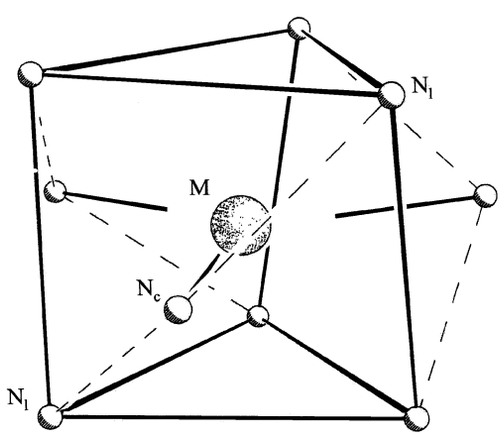

Fig. 1 Line-drawing showing the tricapped-trigonal-prismatic coordination of the complexes. In the $[M(terpy)_3]^{3+}$ cations, N_c are N(2) and N(5) and N_l are N(1), N(3) and N(4); in the $[M(Rbtp)_3]^{3+}$ cations, N_c are N(1) and N_l are N(3) and N(6). N atoms pertaining to the same ligand are joined by dashed lines.

The tris(terpy) complexes

The compounds $[M(terpy)_3]I_3$·2MeCN (M = La, Ce, Nd, U) are isostructural; the structure of the cation in the uranium complex is shown in Fig. 2. The $[M(terpy)_3]^{3+}$ cations possess a two fold axis of symmetry passing through M and N(5) and thus contain 1.5 distinct terpy ligands. The complete list of the M–N_c and M–N_l bond lengths and the N_l–M–N_c and N_l–M–N_l angles is given in Table 1; the M–N_c and M–N_l bond lengths for each terpy ligand are reported in Fig. 3 as a function of the ionic radii of the metals.[21] In the terpy ligand defined by N(1), N(2) and N(3), the M–N_c [M–N(2)] bond lengths are systematically longer than the M–N_l bond lengths [M–N(1) and M–N(3)] whereas the reverse situation is found in the other terpy ligand [M–N(5) < M–N(4)]. The M–N_c bond lengths are almost

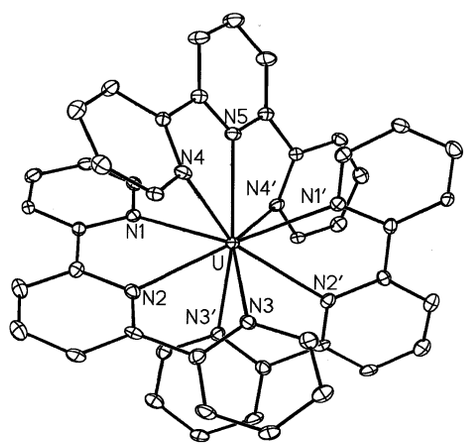

Fig. 2 Perspective view of the cation $[U(terpy)_3]^{3+}$ in **4**·2MeCN with displacement ellipsoids at the 30% probability level (symmetry code: $1 - x, y, 1.5 - z$).

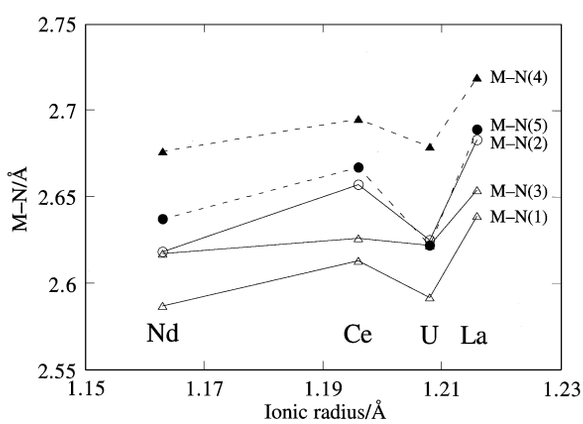

Fig. 3 M–N_c (circles) and M–N_l (triangles) bond lengths in the $[M(terpy)_3]^{3+}$ cations as a function of the metal ionic radii. Open symbols: terpy ligand defined by N(1), N(2) and N(3); closed symbols: terpy ligand defined by N(4) and N(5). Lines are guides for the eye.

Table 2 Selected bond lengths (Å) and angles (°) in the tris(Rbtp) complexes

	[La(Mebtp)$_3$][OTf]$_3$·MeCN **8**·MeCN	[Ce(Mebtp)$_3$][OTf]$_3$·MeCN **9**·MeCN	[Ce(Mebtp)$_3$][OTf]$_2$I·2py **10**·2py	[Ce(Pr^{n}btp)$_3$]I$_3$·3py[a] **6**·3py	[U(Pr^{n}btp)$_3$]I$_3$·4py[a] **7**·4py
M–N(1A)	2.646(7)	2.620(8)	2.668(7)	2.63(2)	2.56(2)
M–N(3A)	2.629(6)	2.605(6)	2.609(8)	2.57(2)	2.54(2)
M–N(6A)	2.624(6)	2.619(6)	2.595(8)	2.64(2)	2.57(3)
M–N(1B)	2.686(6)	2.658(6)	2.626(9)	2.65(1)	2.53(2)
M–N(3B)	2.655(7)	2.625(7)	2.629(8)	2.66(2)	2.56(2)
M–N(6B)	2.651(8)	2.620(7)	2.628(8)	2.61(2)	2.53(3)
M–N(1C)	2.675(7)	2.633(8)	2.655(9)	2.65(2)	2.56(2)
M–N(3C)	2.617(6)	2.611(7)	2.600(9)	2.54(2)	2.52(3)
M–N(6C)	2.608(7)	2.573(7)	2.609(8)	2.59(2)	2.53(3)
⟨M–N$_c$⟩	2.67(2)	2.64(2)	2.65(2)	2.64(1)	2.55(2)
⟨M–N$_l$⟩	2.63(2)	2.61(2)	2.61(1)	2.60(4)	2.54(2)
N(1A)–M–N(3A)	62.0(2)	62.8(2)	61.7(3)	60.4(7)	65.1(9)
N(1A)–M–N(6A)	61.6(2)	61.6(2)	60.8(3)	64.5(7)	62.2(9)
N(3A)–M–N(6A)	123.5(2)	124.4(2)	122.4(3)	124.9(7)	127.3(9)
N(1B)–M–N(3B)	61.2(2)	61.7(2)	61.8(3)	63.8(7)	63.2(9)
N(1B)–M–N(6B)	61.1(2)	61.3(2)	61.8(3)	60.1(7)	63.7(8)
N(3B)–M–N(6B)	122.3(2)	122.9(2)	123.6(3)	123.9(5)	126.8(9)
N(1C)–M–N(3C)	61.3(2)	61.6(2)	61.6(3)	62.2(7)	63.8(9)
N(1C)–M–N(6C)	61.0(2)	62.1(2)	62.0(3)	62.3(6)	63.2(9)
N(3C)–M–N(6C)	122.2(2)	123.7(2)	123.5(3)	124.5(8)	127.0(9)
$\theta_{c,l}$[b]	9.0(5), 11.3(5)	9.7(6), 10.7(5)	10.9(6), 6.8(6)	3.2(16), 2.5(16)	8.8(22), 1.7(25)
	5.6(5), 12.1(4)	6.2(5), 12.7(5)	11.7(6), 11.8(7)	12.9(16), 9.5(16)	5.3(20), 10.8(19)
	8.5(4), 1.8(5)	7.6(4), 2.0(5)	3.9(6), 6.9(5)	1.6(16), 11.1(16)	12.5(18), 6.0(18)
$\theta_{l,l}$[c]	14.8(5), 8.3(5), 9.9(4)	15.3(5), 6.6(5), 9.6(4)	11.4(6), 19.8(6), 10.5(5)	5.5(15), 4.8(15), 9.6(15)	8.1(23), 8.9(19), 11.7(18)

[a] See ref. 10. [b] The two, successive $\theta_{c,l}$ angles in the Rbtp ligands A, B and C. [c] The successive $\theta_{l,l}$ angles of the Rbtp ligands A, B and C.

identical in both ligands, differing by less than 0.02 Å, but the difference between the two average M–N$_l$ bond lengths is equal to 0.07 Å. The differences between the M–N distances in each terpy ligand can be related to the distinct dihedral angles between the pyridine rings. When M–N$_c$ > M–N$_l$, the dihedral angles $\theta_{c,l}$ between the central and lateral pyridine rings are equal to *ca.* 4 and 18°, and the dihedral angle $\theta_{l,l}$ between the two lateral pyridine rings is equal to *ca.* 20° (Table 1); the angles $\theta_{c,l}$ and $\theta_{l,l}$ are much larger, being equal to 24 and 47° respectively, when M–N$_c$ < M–N$_l$ and concomitantly, the N$_l$–N$_l$ distance of 4.72 Å is longer by *ca.* 0.09 Å. These variations clearly show the relation between the lengthening of the M–N$_l$ bonds and the distortion of the terpy ligand.

In the trigonal structure of [Ce(terpy)$_3$]I$_3$·3MeCN (**2**·3MeCN), the M–N$_c$ and M–N$_l$ bond lengths are equal to 2.674(7) and 2.646(5) Å respectively and are close to the average M–N$_c$ and M–N$_l$ bond lengths in **2**·2MeCN [2.662(7) and 2.64(4) Å]. The dihedral angles $\theta_{c,l}$ and $\theta_{l,l}$ of 16 and 32° and the N$_l$–N$_l$ distance of 4.69 Å are intermediate between those determined in each terpy ligand of **2**·2MeCN. The structures of the acetonitrile solvates of **2** can also be compared with that of [Ce(terpy)$_3$][ClO$_4$]$_3$·MeCN in which the M–N$_c$ is shorter than the M–N$_l$ bond distances in two terpy ligands, and is comprised between the M–N$_l$ bond lengths in the third one, while the $\theta_{l,l}$ angles are comprised between 33.5 and 43.7°.[13] The M–N bond lengths in the perchlorate derivative vary from 2.622(6) to 2.679(8) Å and are in the range of the M–N bond lengths in **2**·2MeCN.

Comparison of the M–N$_c$ and M–N$_l$ bond lengths in each terpy ligand of the isostructural complexes [M(terpy)$_3$]I$_3$·2MeCN (M = La, Ce, Nd) shows that the almost linear variation La–N > Ce–N > Nd–N corresponds perfectly to the difference in ionic radii of the trivalent lanthanide ions (Fig. 3).[21] However, the U–N bond lengths in **4**·2MeCN are shorter than those expected from a purely ionic bonding model, by *ca.* 0.05 and 0.03 Å for the U–N$_c$ and U–N$_l$ bond lengths, respectively. It should be noted here that these differences seem significant and can be considered with confidence as they have been measured from a series of isostructural compounds, the crystal structures of which are all of good quality (R_1 = 0.0272–0.0402). It is noteworthy that the shortening of the U–N bond lengths is larger than the difference due to the variation of the ionic radii of the lanthanide ions, which is nicely reflected in the variation of the Ln–N bond distances. The same variations are observed in Fig. 3 when the mean values of the M–N$_c$ and M–N$_l$ bond lengths of both terpy ligands are considered: the ⟨Ln–N⟩ bond lengths vary by following the order of the ionic radii of Ln^{3+} while the ⟨U–N$_c$⟩ and ⟨U–N$_l$⟩ bond lengths deviate from the ionic radii summation by −0.05 and −0.03 Å, respectively. It is interesting to note that ⟨M–N$_c$⟩ is greater than ⟨M–N$_l$⟩ for M = La and Ce, whereas these distances are equal for M = Nd and U.

The tris(Rbtp) complexes

In the crystal structures of [Ce(Pr^{n}btp)$_3$]I$_3$·3py (**6**·3py), [U(Pr^{n}btp)$_3$]I$_3$·4py (**7**·4py), [La(Mebtp)$_3$][OTf]$_3$·MeCN (**8**·MeCN), [Ce(Mebtp)$_3$][OTf]$_3$·MeCN (**9**·MeCN) and [Ce(Mebtp)$_3$][OTf]$_2$I·2py (**10**·2py), practically no difference is observed in the coordination of the Rbtp molecules. The M–N bond lengths and N–M–N angles are reported in Table 2; the structure of the $[Ce(Mebtp)_3]^{3+}$ cation in **9**·MeCN is shown in Fig. 4. The M–N$_c$ bond length is greater than or equal to the M–N$_l$ bond lengths in the three distinct Rbtp ligands of each compound; this trend is particularly noticeable in the two isostructural complexes **8**·MeCN and **9**·MeCN. In the three cerium complexes, the M–N$_c$ bond lengths are ranging from 2.620(8) to 2.668(7) Å with a mean value of 2.64(2) Å, and the M–N$_l$ bond lengths lie between 2.54(2) and 2.66(2) Å and average 2.61(7) Å. It is noteworthy that the different alkyl groups at the 5 and 6 positions of the triazine rings have no significant effect on the metal coordination sphere. The Rbtp ligands appear to be much less distorted than terpy in the $[M(terpy)_3]^{3+}$ cations since the $\theta_{c,l}$ and $\theta_{l,l}$ dihedral angles are lower than 13 and 20°, and average 8 and 11°, respectively. Quite similar distortions of the Mebtp ligands were observed in the crystal structure of [Sm(Mebtp)$_3$][Sm(NO$_3$)$_5$]$_{1.5}$; in this samarium compound, the average Sm–N$_c$ and Sm–N$_l$ bond lengths are both equal to

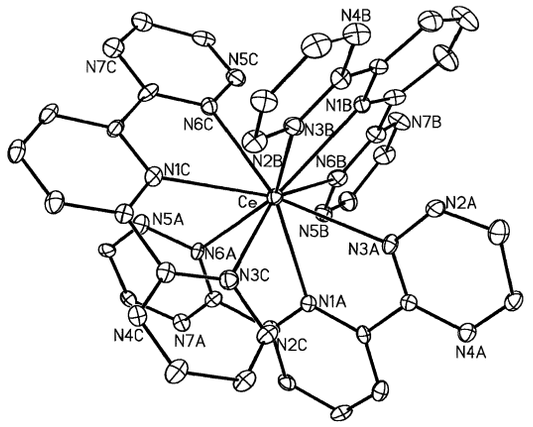

Fig. 4 Perspective view of the cation $[Ce(Mebtp)_3]^{3+}$ in **9**·MeCN with displacement ellipsoids at the 30% probability level.

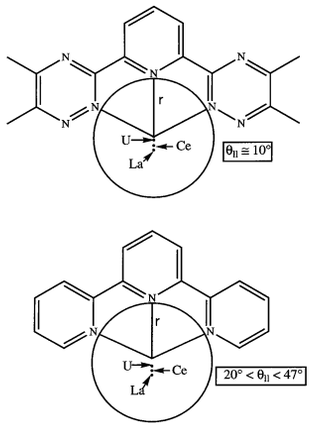

Fig. 6 Respective positions of the La, Ce and U atoms inside the cavity of the terpy and Mebtp ligands.

2.57(2) Å.[18] As in the case of the $[Ln(terpy)_3]^{3+}$ cations, the average $M–N_c$ and $M–N_l$ bond lengths in the $[Ln(Rbtp)_3]^{3+}$ cations (Ln = La, Ce, Sm) follow the order La–N > Ce–N > Sm–N, that is in good agreement with the variation of the ionic radii of the trivalent 4f ions (Fig. 5). Here again, the $U–N_c$ and

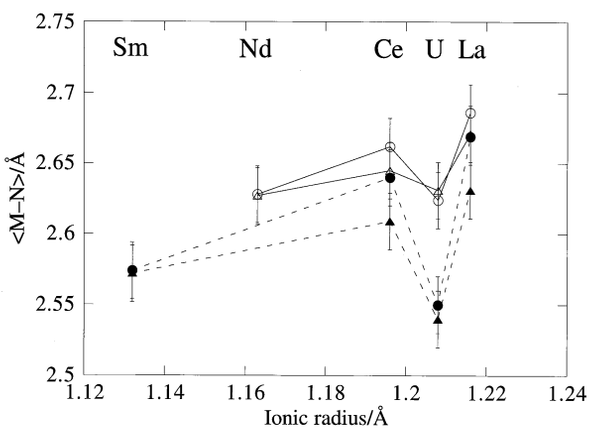

Fig. 5 Mean values of $M–N_c$ (circles) and $M–N_l$ (triangles) bond lengths in the $[M(terpy)_3]^{3+}$ (open symbols) and $[M(Rbtp)_3]^{3+}$ (closed symbols) cations. Standard deviations indicated as vertical bars. Lines are guides for the eye.

$U–N_l$ bond lengths in the $[U(Pr^nbtp)_3]^{3+}$ cation are significantly shorter than those expected from a purely ionic bonding model, by 0.11 and 0.08 Å respectively.

Differences in the structural parameters of the tris(terpy) and tris(Rbtp) complexes

In order to visualize the position of the metal centre inside the cavity of terpy and Rbtp, it is helpful to consider the circle passing through the three coordinating nitrogen atoms in a planar ligand, as shown in Fig. 6. In the Rbtp complexes, the terdentate ligand is indeed only slightly distorted and the $Ln–N_c$ are longer than the $Ln–N_l$ bond lengths, indicating that the Ln–N bond lengths are longer than the radius *r* of the circle. The uranium atom in the $[U(Pr^nbtp)_3]^{3+}$ cation is closely lying on the centre of this circle since the $U–N_c$ and $U–N_l$ bond lengths are almost equal. In the $[M(terpy)_3]^{3+}$ cations, the $M–N_c$ are longer than the $M–N_c$(Rbtp) bond lengths and are thus longer than the radius of the circle passing through N(1), N(3) and N(6), by considering that the N_3 cavities of terpy and Rbtp have the same size. The $M–N_c$(terpy) are therefore expected to be longer than the $M–N_l$(terpy) bond lengths if the terpy ligand is planar, but this is not the case in one of the two terpy ligands because of the great distortion of the ligand which moves the lateral nitrogen atoms away from the metal centre. It is also interesting to note that the value for which the $Ln–N_c$ and $Ln–N_l$ bond lengths are equal or, in other words, the value for which the ratio $Ln–N_c/Ln–N_l$ is inverted, seems to be greater for terpy than for Rbtp, being equal to 2.63 and 2.57 Å respectively; a value of 2.58 Å was found in the series of the lanthanide mono(terpy) compounds.[22] This difference would indicate that the nitrogen cavity of the Rbtp ligand is slightly smaller than that of terpy, in agreement with the fact that the average $N_l–C$ bond distance of 1.33(3) Å in the Rbtp ligand is *ca.* 0.03 Å shorter than the corresponding distance in terpy.

Fig. 5 clearly shows that for any given metal, the M–N(Rbtp) bond lengths are shorter than the M–N(terpy) bond lengths and for any given ligand, Rbtp or terpy, the uranium–nitrogen bond distances are shorter than the lanthanide–nitrogen bond lengths and this shortening is more important with Rbtp than with terpy. This trend corresponds to the better affinity and selectivity of Rbtp, in comparison with terpy, in the complexation of trivalent 4f and 5f ions.[11] The remarkably higher performances of the Rbtp *vs.* terpy ligands obviously result from the replacement in terpy of the two lateral pyridine rings with two less basic and less electron rich 2,3,4-triazine moieties. As shown by recent quantum chemical calculations, such terdentate planar ligands in which the central and lateral nitrogen atoms have significantly different effective charges are very efficient in the complexation of trivalent lanthanide ions because they ensure both a good donation from the ligand to the cation and a good back donation from the cation to the ligand.[23] The high selectivity of these ligands in the An(III)/Ln(III) separation should be related to the presence of a stronger π back-bonding interaction between the trivalent 5f ion and the aromatic nitrogen ligand.

Conclusion

Crystallographic studies have demonstrated that the variation of the metal–nitrogen bond lengths in the $[M(terpy)_3]^{3+}$ and $[M(Rbtp)_3]^{3+}$ cations (M = La, Ce and U) reflects perfectly the better performances of Rbtp relative to terpy in both the coordinating ability towards 4f and 5f ions and selective complexation of U(III) over La(III) or Ce(III) in solution. Thus, the M–N(Rbtp) bond lengths are shorter than the M–N(terpy) bond lengths and the U–N bond lengths are shorter than the corresponding La–N or Ce–N bond distances. The deviation of the U–N bond lengths from a purely ionic bonding model is consistent with the presence of a stronger π back-bonding interaction between the U(III) ion and the terdentate ligand.

Experimental

All preparations and experiments were carried out under argon (< 5 ppm oxygen or water) using standard Schlenk-vessel and vacuum-line techniques or in a glove box. Solvents were thoroughly dried and deoxygenated by standard methods and distilled immediately before use; deuterated pyridine (Eurisotop) was distilled over NaH and stored over 3 Å molecular sieves, and deuterated acetonitrile was dried over 3 Å molecular sieves. Terpyridine (Aldrich) was dried under vacuum; Mebtp and Pr^{n}btp were prepared by a published method.[18] The lanthanide iodides and triflates (Aldrich) were dried under vacuum; $[UI_3(py)_4]$[24] and $U(OTf)_3$[25] were prepared by published methods.

Elemental analyses were performed by Analytische Laboratorien at Lindlar (Germany). The ^{1}H NMR spectra were recorded on a Bruker DPX 200 instrument and referenced internally using the residual protio solvent resonances relative to tetramethylsilane (δ 0).

Preparations

$[La(terpy)_3]I_3$ 1. An NMR tube was charged with terpy (27.0 mg, 0.11 mmol), LaI_3 (20.0 mg, 0.038 mmol) and acetonitrile (2 cm^3). The mixture was heated for 2 h at 100 °C. The solution was discarded *via* a micropipette and orange crystals of **1** were obtained after drying under vacuum (40 mg, 85%) (Found: C, 44.15; H, 2.94; N, 10.55. $C_{45}H_{33}LaI_3N_9$ requires C, 44.32; H, 2.72; N, 10.33%). $\delta_H(CD_3CN)$ 8.92 (2 H, br d,), 8.4 (5 H, m), 8.13 (2 H, d of t, *J* 8 and 1.5 Hz), 7.45 (2 H, t, *J* 8 Hz).

$[Ce(terpy)_3]I_3$ 2. A round-bottom flask (25 cm^3) was charged with terpy (67.5 mg, 0.29 mmol) and CeI_3 (50.0 mg, 0.096 mmol) and acetonitrile (20 cm^3) was condensed into it at −78 °C under vacuum. The mixture was heated for 2 h at 100 °C. The orange microcrystalline powder of **2** was filtered off and dried under vacuum (96.0 mg, 81%) (Found: C, 44.14; H, 2.85; N, 10.49. $C_{45}H_{33}CeI_3N_9$ requires C, 44.28; H, 2.72; N, 10.32%). $\delta_H(CD_3CN)$ 10.40 (4 H, br t, *J* 8 Hz), 10.11 (1 H, t, *J* 7.5 Hz), 8.80 (2 H, t, *J* 8 Hz), 6.45 (2 H, d, *J* 7.5 Hz), 2.26 (2 H, br s).

$[Nd(terpy)_3]I_3$ 3. By using the same procedure as for **2**, reaction of terpy (66.6 mg, 0.28 mmol) and NdI_3 (50.0 mg, 0.095 mmol) gave an orange microcrystalline powder of **3** (91.0 mg, 78%) (Found: C, 43.97; H, 2.77; N, 10.36. $C_{45}H_{33}I_3N_9Nd$ requires C, 44.13; H, 2.71; N, 10.29%). $\delta_H(CD_3CN)$ 11.71 (4 H, br t, *J* 8 Hz), 10.52 (1 H, t, *J* 7.5 Hz), 8.88 (2 H, t, *J* 8 Hz), 7.39 (2 H, d, *J* 7.5 Hz), 2.47 (2 H, br s).

$[U(terpy)_3]I_3$ 4. An NMR tube was charged with terpy (15.0 mg, 0.064 mmol), $[UI_3(py)_4]$ (20.0 mg, 0.021 mmol) and acetonitrile (2 cm^3). After 2.5 h at room temperature, the solution was discarded *via* a micropipette and the dark green powder of **4** was washed with toluene (3 cm^3) and dried under vacuum (24.0 mg, 85%) (Found: C, 40.81; H, 2.72; N, 9.80. $C_{45}H_{33}I_3N_9U$ requires C, 40.99; H, 2.52; N, 9.56%). Because of the insolubility of **4**, the NMR spectrum could not be recorded.

$[Ce(Mebtp)_3]I_3$ 5. An NMR tube was charged with Mebtp (33.8 mg, 0.11 mmol), CeI_3 (20.0 mg, 0.038 mmol) and pyridine (2 cm^3). The mixture was heated at 100 °C and an orange solution was obtained. The orange powder of **5** precipitated upon addition of diethyl ether (3 cm^3). The solution was discarded *via* a micropipette and the powder was washed with toluene (3 cm^3) and dried under vacuum (50.2 mg, 93%) (Found: C, 38.83; H, 3.36; N, 20.73. $C_{45}H_{45}CeI_3N_{21}$ requires C, 38.58; H, 3.24; N, 20.99%); $\delta_H(C_6D_5N)$ 12.28 (2 H, d, *J* 7 Hz, 3,5-py), 11.91 (1 H, t, *J* 7 Hz, 4-py), 0.55 (6 H, s, Me), −0.41 (6 H, s, Me); $\delta_H(CD_3CN)$ 11.92 (2 H, d, *J* 7 Hz, 3,5-py), 11.38 (1 H, t, *J* 7 Hz, 4-py), 1.32 (6 H, s, Me), 0.07 (6 H, s, Me).

$[U(Mebtp)_3]I_3$. An NMR tube was charged with Mebtp (9.4 mg, 0.03 mmol) and $[UI_3(py)_4]$ (10.0 mg, 0.01 mmol) in C_6D_5N (0.4 cm^3). The spectrum of the brown solution showed the immediate and quantitative formation of $[U(Mebtp)_3]I_3$. $\delta_H(C_6D_5N)$ 33.95 (1 H, t, *J* 7 Hz, 4-py), 5.64 (2 H, 2, *J* 7 Hz, 3,5-py), 4.59 (6 H, s, Me), −18.04 (6 H, s, Me).

$[Ce(Pr^nbtp)_3]I_3$ 6 and $[U(Pr^nbtp)_3]I_3$ 7. These complexes were characterized only by the crystal structure of their pyridine solvates **6**·3py and **7**·4py which were obtained by slow diffusion of pentane into pyridine solutions of CeI_3 or $[UI_3(py)_4]$ and Pr^{n}btp in the 1 : 3 molar ratio.

$[La(Mebtp)_3][OTf]_3$ 8. An NMR tube was charged with Mebtp (15.0 mg, 0.051 mmol), $La(OTf)_3$ (10.0 mg, 0.017 mmol), and pyridine (2 cm^3). The mixture was heated at 110 °C and a colorless solution was obtained. The off-white powder of **8** precipitated upon addition of toluene (3 cm^3). The solution was discarded *via* a micropipette and the powder was washed with toluene (4 cm^3) and dried under vacuum (24.2 mg, 96%) (Found: C, 39.19; H, 3.16; N, 20.23. $C_{48}H_{45}F_9LaN_{21}O_9S_3$ requires C, 39.32; H, 3.09; N, 20.06%); $\delta_H(C_6D_5N)$ 8.99 (2 H, d, *J* 8 Hz, 3,5-py), 8.63 (1 H, t, *J* 8 Hz, 4-py), 2.30 (6 H, s, Me), 2.03 (6 H, s, Me); $\delta_H(CD_3CN)$ 8.88 (2 H, d, *J* 8 Hz, 3,5-py), 8.53 (1 H, t, *J* 8 Hz, 4-py), 2.51 (6 H, s, Me), 2.06 (6 H, s, Me).

$[Ce(Mebtp)_3][OTf]_3$ 9. An NMR tube was charged with Mebtp (22.5 mg, 0.077 mmol), $Ce(OTf)_3$ (15.0 mg, 0.025 mmol) and pyridine (2 cm^3). The mixture was heated at 110 °C and a pale yellow solution was obtained. The solvent was evaporated off and the yellow powder of **9** was washed with THF (4 cm^3) and toluene (4 cm^3) and dried under vacuum (35.1 mg, 94%) (Found: C, 39.11; H, 3.26; N, 19.85. $C_{48}H_{45}CeF_9N_{21}O_9S_3$ requires C, 39.29; H, 3.09; N, 20.04%); $\delta_H(C_6D_5N)$ 11.01 (2 H, d, *J* 8 Hz, 3,5-py), 10.47 (1 H, t, *J* 8 Hz, 4-py), 1.64 (6 H, s, Me), 1.37 (6 H, s, Me); $\delta_H(CD_3CN)$ 10.87 (2 H, d, *J* 8 Hz, 3,5-py), 10.35 (1 H, t, *J* 8 Hz, 4-py), 1.88 (6 H, s, Me), 1.31 (6 H, s, Me). The ^{1}H NMR spectra of a pyridine solution containing a 1 : 1 mixture of **5** and **9** or a 1 : 3 mixture of **5** and KOTf exhibits signals at $\delta_H(C_6D_5N)$ 11.35 (2 H, d, *J* 8 Hz, 3,5-py), 10.91 (1 H, t, *J* 8 Hz, 4-py), 1.41 (6 H, s, Me), 0.95 (6 H, s, Me).

$[U(Mebtp)_3][OTf]_3$ 11. An NMR tube was charged with Mebtp (19.3 mg, 0.066 mmol), $U(OTf)_3$ (15.0 mg, 0.022 mmol), and pyridine (2 cm^3). After 12 h at room temperature, a dark blue–green solution was obtained. The grey–blue powder of **11** precipitated upon addition of toluene (3 cm^3). The solution was discarded *via* a micropipette and the powder was washed with toluene (3 cm^3) and dried under vacuum (24.3 mg, 71%) (Found: C, 37.01; H, 3.01; N, 18.73. $C_{48}H_{45}F_9N_{21}O_9S_3U$ requires C, 36.83; H, 2.89; N, 18.79%); $\delta_H(CD_3CN)$ 32.20 (1 H, t, *J* 7 Hz, 4-py), 6.37 (2 H, d, *J* 7 Hz, 3,5-py), 4.60 (6 H, s, Me), −17.02 (6 H, s, Me).

Crystallography

Both orange and yellow crystals of solvates of **1**–**3** were deposited from acetonitrile solutions of the complexes upon heating for *ca.* 1–10 h at 110 °C; these crystals were found to contain respectively 2 and 3 molecules of solvent per metal. Dark green crystals of **4**·2MeCN were obtained in a similar fashion, together with an ochre powder of an oxidation product. Orange crystals of acetonitrile solvates of **8** and **9** were obtained by slow diffusion of diethyl ether into acetonitrile solutions of the compounds. Diffraction collections were carried out on a Nonius Kappa–CCD diffractometer. The lattice parameters were determined from ten images recorded

Table 3 Crystallographic data of the tris(terpy) complexes

	$[La(terpy)_3]I_3\cdot 2MeCN$ **1**·2MeCN	$[Ce(terpy)_3]I_3\cdot 2MeCN$ **2**·2MeCN	$[Ce(terpy)_3]I_3\cdot 3MeCN$ **2**·3MeCN	$[Nd(terpy)_3]I_3\cdot 2MeCN$ **3**·2MeCN	$[U(terpy)_3]I_3\cdot 2MeCN$ **4**·2MeCN
Chemical formula	$C_{49}H_{39}I_3LaN_{11}$	$C_{49}H_{39}CeI_3N_{11}$	$C_{51}H_{42}CeI_3N_{12}$	$C_{49}H_{39}I_3N_{11}Nd$	$C_{49}H_{39}I_3N_{11}U$
M/g mol^{-1}	1301.52	1302.73	1343.79	1306.85	1400.64
Crystal system	orthorhombic	orthorhombic	trigonal	orthorhombic	orthorhombic
Space group	*Pcca*	*Pcca*	*R*32	*Pcca*	*Pcca*
a/Å	19.107(4)	19.149(4)	12.6180(18)	19.220(4)	19.198(4)
b/Å	16.659(3)	16.626(3)	12.6180(18)	16.591(3)	16.591(3)
c/Å	14.724(3)	14.709(3)	27.903(6)	14.685(3)	14.677(3)
V/Å^3	4686.7(16)	4682.9(16)	3847.4(11)	4682.7(16)	4674.8(16)
Z	4	4	3	4	4
ρ_{calcd}/g cm^{-3}	1.845	1.848	1.740	1.854	1.990
μ (MoKα)/mm^{-1}	2.935	2.998	2.740	3.134	5.501
Crystal size/mm	0.25 × 0.15 × 0.10	0.15 × 0.10 × 0.10	0.20 × 0.15 × 0.10	0.15 × 0.10 × 0.05	0.15 × 0.10 × 0.02
T_{min}/T_{max}	0.580/0.761	0.625/0.762	0.610/0.801	0.460/0.540	0.378/0.458
F(000)	2504	2508	1947	2516	2644
2θ range/°	5–49	5–49	7–49	5–49	6–51
T/K	123(2)	123(2)	123(2)	123(2)	123(2)
No. of data collected	29196	29630	7985	29212	30940
No. of unique data	3941	3946	1362	3953	4324
Observed data [$I > 2\sigma(I)$]	3320	3235	1316	3270	3334
R_{int}	0.064	0.073	0.025	0.075	0.082
No. of parameters	291	291	108	291	291
R_1 [a]	0.027	0.029	0.033	0.029	0.040
wR_2 [b]	0.059	0.067	0.081	0.063	0.090
S	1.033	1.013	1.029	1.022	1.010
$\Delta\rho_{min}$/e Å^{-3}	−0.59	−0.59	−0.82	−0.64	−0.91
$\Delta\rho_{max}$/e Å^{-3}	0.80	0.65	0.81	0.87	0.87

[a] $R_1 = \Sigma||F_o| - |F_c||/|F_o|$ (observed reflections). [b] $wR_2 = [\Sigma w(|F_o^2| - |F_c^2|)^2/\Sigma w|F_o^2|^2]^{1/2}$ (observed reflections).

Table 4 Crystallographic data of the tris(Mebtp) complexes

	$[La(Mebtp)_3][OTf]_3\cdot MeCN$ **8**·MeCN	$[Ce(Mebtp)_3][OTf]_3\cdot MeCN$ **9**·MeCN	$[Ce(Mebtp)_3][OTf]_2I\cdot 2py$ **10**·2py
Chemical formula	$C_{50}H_{48}F_9LaN_{22}O_9S_3$	$C_{50}H_{48}CeF_9N_{22}O_9S_3$	$C_{57}H_{55}CeF_6IN_{23}O_6S_2$
M/g mol^{-1}	1507.19	1508.40	1603.38
Crystal system	monoclinic	monoclinic	monoclinic
Space group	$P2_1$	$P2_1$	$P2_1$
a/Å	13.337(3)	13.240(3)	13.254(3)
b/Å	17.283(4)	17.266(4)	17.234(3)
c/Å	14.449(3)	14.491(3)	14.747(3)
β/°	104.29(3)	103.81(3)	103.19(3)
V/Å^3	3227.5(13)	3217.0(13)	3279.6(11)
Z	2	2	2
ρ_{calcd}/g cm^{-3}	1.551	1.557	1.624
μ (MoKα)/mm^{-1}	0.854	0.901	1.313
Crystal size/mm	0.15 × 0.10 × 0.05	0.20 × 0.15 × 0.10	0.15 × 0.10 × 0.05
T_{min}/T_{max}	0.801/0.920	0.789/0.870	0.608/0.799
F(000)	1520	1522	1606
2θ range/°	6–49	6–49	6–49
T/K	123(2)	123(2)	123(2)
No. of data collected	20084	20089	20350
No. of unique data	10086	10154	10994
Observed data [$I > 2\sigma(I)$]	8529	8669	8283
R_{int}	0.066	0.075	0.075
No. of parameters	832	859	839
R_1 [a]	0.055	0.056	0.063
wR_2 [b]	0.124	0.135	0.129
S	1.030	0.990	1.010
Flack parameter	−0.006(16)	−0.001(16)	0.04(2)
$\Delta\rho_{min}$/e Å^{-3}	−0.52	−0.64	−0.85
$\Delta\rho_{max}$/e Å^{-3}	0.82	0.85	0.93

[a] $R_1 = \Sigma||F_o| - |F_c||/|F_o|$ (observed reflections). [b] $wR_2 = [\Sigma w(|F_o^2| - |F_c^2|)^2/\Sigma w|F_o^2|^2]^{1/2}$ (observed reflections).

with 2° Φ-scans and later refined on all data. A 180° Φ-range was scanned with 2° steps with a crystal to detector distance fixed at 30 mm. Absorption effects were corrected empirically with the program MULABS from PLATON.[26] The structures were solved by the heavy atom method and refined by full matrix least-squares on F^2 with anisotropic thermal parameters for all non-H atoms. H atoms were introduced at calculated positions and constrained to ride on their parent C atom with an isotropic displacement parameter equal to 1.2 (CH) or 1.5 (CH_3) times that of the parent atom. In the structure of **2**·3MeCN, the solvent molecules were found disordered on two positions with 0.5 occupancy factors. In the structure of **10**·2py, the two pyridine solvent molecules were constrained to fit a regular hexagon with an anisotropic displacement parameter for each pyridine ring. All calculations were performed on an O2 Silicon Graphics Station with the SHELXTL package.[27]

Crystal data and summary of data collection and refinement for the tris(terpy) and tris(Mebtp) complexes are given in Tables 3 and 4, respectively.

CCDC reference numbers 181672–181679.

See http://www.rsc.org/suppdata/dt/b2/b203725d/ for crystallographic data in CIF or other electronic format.

Acknowledgements

The authors thank Dr. C. Rivière for training one of us (P. B. I.) for the manipulation of air sensitive products, and Dr. D. Guillaneux for the supply of the Rbtp ligands.

References

1 C. Piguet and J.-C. G. Bünzli, *Chem. Soc. Rev.*, 1999, **28**, 347.
2 *Handbook on the Physics and Chemistry of Rare Earths. Lanthanides/Actinides: Chemistry*, ed. K. A. Gschneidner, Jr., L. Eyring, G. R. Choppin and G. H. Lander, Elsevier Science, Amsterdam, 1994, vol. 18.
3 *Actinides and Fission Products Partitioning and Transmutation. Status and assessment Report*, NEA/OECD Report, NEA/OECD, Paris, 1999; *Actinides and Fission Products Partitioning and Transmutation*. Proceedings of the Fifth International Information Exchange Meeting, Mol, Belgium, 25–27 Nov. 1998; *NEA/OECD Report*, NEA/OECD, Paris, 1999.
4 K. L. Nash, *Solvent Extr. Ion Exch.*, 1993, **11**, 729; K. L. Nash, in *Handbook on the Physics and Chemistry of Rare Earths. Lanthanides/Actinides: Chemistry*, ed. K. A. Gschneidner, Jr., L. Eyring, G. R. Choppin and G. H. Lander, Elsevier Science, Amsterdam, 1994, vol. 18, p. 197.
5 J. G. Brennan, S. D. Stults, R. A. Andersen and A. Zalkin, *Organometallics*, 1988, **7**, 1329.
6 M. del Mar Conejo, J. S. Parry, E. Carmona, M. Schultz, J. G. Brennan, S. M. Beshouri, R. A. Andersen, R. D. Rogers, S. Coles and M. Hursthouse, *Chem. Eur. J.*, 1999, **5**, 3000.
7 L. Jiacheng, S. Zhigang, W. Liufang, Z. Jinzhong and H. Xiaoying, *Acta Chem. Scand.*, 1999, **53**, 90.
8 R. Wietzke, M. Mazzanti, J. M. Latour and J. Pécaut, *J. Chem. Soc., Dalton Trans.*, 2000, 4167.
9 C. Rivière, M. Nierlich, M. Ephritikhine and C. Madic, *Inorg. Chem.*, 2001, **40**, 4428.
10 P. B. Iveson, C. Rivière, D. Guillaneux, M. Nierlich, P. Thuéry, M. Ephritikhine and C. Madic, *Chem. Commun.*, 2001, 1512.
11 Z. Kolarik, U. Mullich and F. Gassner, *Solv. Extr. Ion Exch.*, 1999, **17**, 23; Z. Kolarik, U. Mullich and F. Gassner, *Solv. Extr. Ion Exch.*, 1999, **17**, 1155.
12 J. C. Berthet, C. Rivière, Y. Miquel, M. Nierlich, C. Madic and M. Ephritikhine, *Eur. J. Inorg. Chem.*, 2002, 1439.
13 L. I. Semenova, A. N. Sobolev, B. W. Skelton and A. H. White, *Aust. J. Chem.*, 1999, **52**, 519.
14 R. D. Chapman, R. T. Loda, J. P. Riehl and R. W. Schwartz, *Inorg. Chem.*, 1984, **23**, 1652; D. A. Durham, G. H. Frost and F. A. Hart, *J. Inorg. Nucl. Chem.*, 1969, **31**, 833.
15 H. R. Mürner, E. Chassat, R. P. Thummel and J.-C. G. Bünzli, *J. Chem. Soc., Dalton Trans.*, 2000, 2809.
16 C. Mallet, R. P. Thummel and C. Hery, *Inorg. Chim. Acta*, 1993, **210**, 223.
17 J.-C. Berthet, M. Lance, M. Nierlich and M. Ephritikhine, *Eur. J. Inorg. Chem.*, 2000, 1969.
18 M. G. B. Drew, D. Guillaneux, M. J. Hudson, P. B. Iveson, M. L. Russell and C. Madic, *Inorg. Chem. Commun.*, 2001, **4**, 12; F. H. Case, *J. Heterocycl. Chem.*, 1971, **8**, 1043.
19 M. G. B. Drew, D. Guillaneux, M. J. Hudson, P. B. Iveson and C. Madic, *Inorg. Chem. Commun.*, 2001, **4**, 462.
20 D. L. Kepert, *Inorganic Stereochemistry* (Inorganic Chemistry Concepts, vol. 6), Springer Verlag, Berlin–Heidelberg–New York, 1982.
21 E. N. Rizkalla and G. R. Choppin, in *Handbook on the Physics and Chemistry of Rare Earths. Lanthanides/Actinides: Chemistry*, ed. K. A. Gschneidner, Jr., L. Eyring, G. R. Choppin and G. H. Lander, Elsevier Science, Amsterdam, 1994, vol. 18, p. 529.
22 M. G. B. Drew, P. B. Iveson, M. J. Hudson, J. O. Liljenzin, L. Spjuth, P. Y. Cordier, A. Enarsson, C. Hill and C. Madic, *J. Chem. Soc., Dalton Trans.*, 2000, 821.
23 G. Ionova, C. Rabbe, R. Guillaumont, S. Ionov, C. Madic, J. C. Krupa and D. Guillaneux, *New J. Chem.*, 2002, **26**, 234.
24 L. R. Avens, S. G. Bott, D. L. Clark, A. P. Sattelberger, J. G. Watkin and B. D. Zwick, *Inorg. Chem.*, 1994, **33**, 2248.
25 J.-C. Berthet, M. Lance, M. Nierlich and M. Ephritikhine, *Eur. J. Inorg. Chem.*, 1999, 2005.
26 A. L. Spek, MULABS, PLATON, University of Utrecht, The Netherlands, 1998.
27 G. M. Sheldrick, SHELXTL, University of Göttingen, Germany, distributed by Bruker-AXS, Madison, WI, 1999.